

Theory of nonlinear optical properties of small metallic spheres

D. Östling*, P. Stampfli, K.H. Bennemann

Institut für Theoretische Physik, Freie Universität Berlin, Arnimallee 14, D-14195 Berlin, Germany

Received: 31 March 1993 / Final version: 12 April 1993

Abstract. We calculate the nonlinear optical properties of small metallic spheres using electromagnetic theory and assuming that the local response of the conduction electrons is the same as for a plane surface. Electromagnetic Mie-resonances cause a strong increase of the second and higher harmonics in the reflected light. Detailed results are given for the second and third harmonic generation, its dependence on the frequency and polarization of the incident light, and on the cluster size. An enhancement of the second harmonic generation by a factor of about 5000 is obtained for small spherical metallic clusters. This is in good agreement with experiments on artificially roughened metal surfaces.

PACS: 42.65.K; 36.40; 73.35.

1. Introduction

Experiments have shown that the second harmonic generation of light is strongly enhanced at artificially roughened metal surfaces [1], metal island films [2] and microlithographic metal particles [2] in comparison to microscopically smooth metal surfaces. Similar enhancements are found for the third order Kerr nonlinearity of doped glasses [3, 4] containing nanometer metal clusters. To explain qualitatively these enhancements it has been argued that Mie-resonances enhance the local fields at the structures of roughened surfaces [1] and the surface of metal particles [2–4], which increases higher harmonic generation. However, previous theoretical work [3, 5] only applies to metal particles of very small size, such that the quasistatic dipole approximation can be used. But note that the dipole approximation also implies that small metal spheres do not generate second harmonic radiation because of their centrosymmetric shape. Thus we consider

in this work large metallic spheres with a size, which is of the same magnitude as the wavelength of light.

In this work we present a simplified model for nonlinear optics at large metal spheres. Because of the large size, we assume that the nonlinear properties (such as the second order susceptibility χ_2) of the spherical surfaces are the same as for a planar bulk surface. Important differences then only arise because of the Mie-resonances [6–8], which can be directly excited by the incident radiation. These collective resonances strongly increase the local fields at the surface of the sphere and thus the higher harmonic generation. In the present paper we analyze how the different multipolar resonances are nonlinearly combined, taking into account the spherical symmetry of the surface. Further we examine the resulting higher harmonic radiation, which depends strongly on the size of the sphere.

In Chapt. 2 we discuss our theory and in Chapt. 3 detailed results are presented for the second- and third order harmonic generation at large metal spheres. A summary is given in Chapt. 4.

2. Theory

First, we use Mie theory to calculate the linear scattering of light and the induced surface charge σ , which is proportional to the amplitude of the incident radiation. We then assume that a surface charge, which is proportional to the second power of σ , acts as a source for the second harmonic. Similarly the third harmonic is generated by the third power of σ . Electromagnetic theory is used to calculate the response of the metal sphere to this source and to obtain the radiated intensity of the higher harmonic. The result is then compared to the higher harmonic generation of a plane surface calculated using the same model. Note that the conductivity of the metal is large at low frequencies and that the source of the second harmonic induces a compensating charge on the metal surface. Thus the second harmonic is in this case effectively produced by a surface polarization similarly to the

* Permanent address: Department of Physics, Chalmers University of Technology and University of Göteborg, S-41296 Göteborg, Sweden

phenomenological model of other authors [9]. But at higher frequencies metallic screening is incomplete and the effective source of higher harmonic radiation is not restricted to be a surface polarization.

2.1. Mie theory for the incident wave

The Mie theory for scattering of light at a sphere of radius a is well known. Thus we only present the relevant results and omit the details of calculation. Here we explicitly consider only incident waves of circular polarization. Other polarizations (e.g. linear) are obtained using appropriate linear combinations. The electric fields \mathbf{E}_i of the incident wave ($i \equiv \text{inc}$), the scattered wave ($i \equiv \text{sc}$) and the wave inside the sphere ($i \equiv \text{in}$) are expressed with multipole expansions of the form [10]

$$\mathbf{E}_i(\mathbf{x}) = \sum_{l,m} C(l) \left[a_{M,i}(l,m) f_l(kr) \mathbf{X}_{l,m} \pm \frac{a_{E,i}(l,m)}{k} \nabla \times f_l(kr) \mathbf{X}_{l,m} \right], \quad (1)$$

where $\mathbf{X}_{l,m} = -i[l(l+1)]^{-1/2}(\mathbf{r} \times \nabla) Y_{l,m}(\theta, \phi)$ is a vector spherical harmonic, $C(l) = i^l \sqrt{4\pi(2l+1)}$ and $k = \omega/c$. The $a_{M,i}(l,m)$ and $a_{E,i}(l,m)$ are multipole coefficients. For incident waves of positive or negative helicity (corresponding to a respective sign $+$ or $-$), we have $a_{M,\text{inc}}(l, \pm 1) = 1$, $a_{E,\text{inc}}(l, \pm 1) = 1$ and $f_l(kr) = j_l(kr)$ is a spherical Bessel function. Using the appropriate boundary conditions at the surface of the sphere with radius a , we obtain for the scattered wave ($r = a, k_1 = \sqrt{\epsilon(\omega)} k$)

$$a_{M,\text{sc}}(l, \pm 1) = \frac{j_l(kr) \frac{\partial}{\partial r} [r j_l(k_1 r)] - j_l(k_1 r) \frac{\partial}{\partial r} [r j_l(kr)]}{j_l(k_1 r) \frac{\partial}{\partial r} [r h_l^{(1)}(kr)] - h_l^{(1)}(kr) \frac{\partial}{\partial r} [r j_l(k_1 r)]} \Bigg|_{r=a} \quad (2)$$

and

$$a_{E,\text{sc}}(l, \pm 1) = \frac{j_l(kr) \frac{\partial}{\partial r} [r j_l(k_1 r)] - \epsilon(\omega) j_l(k_1 r) \frac{\partial}{\partial r} [r j_l(kr)]}{\epsilon(\omega) j_l(k_1 r) \frac{\partial}{\partial r} [r h_l^{(1)}(kr)] - h_l^{(1)}(kr) \frac{\partial}{\partial r} [r j_l(k_1 r)]} \Bigg|_{r=a} \quad (3)$$

where $f_l(kr) = h_l^{(1)}(kr)$.

As usual we may view the scattered field E_{sc} as generated by the induced surface charge density σ resulting from the component of polarization perpendicular to the sphere. This surface charge density σ is obtained from

$$\sigma(\theta, \phi) = \frac{1}{4\pi} \text{Re}[(1 - \epsilon(\omega)^{-1}) \mathbf{n} \cdot (\mathbf{E}_{\text{inc}} + \mathbf{E}_{\text{sc}})] e^{-i\omega t}, \quad (4)$$

where $\mathbf{n} = \mathbf{r}/|\mathbf{r}|$. Considering the surface-charge density from incident light with positive or negative helicity, using the notation σ_+ and σ_- respectively, we expand in spherical harmonics

$$\sigma_{\pm}(\theta, \phi) = \frac{1}{2} \sum_{l=1}^{\infty} a_{l,\pm 1}^{(1)} Y_{l,\pm 1}(\theta, \phi) e^{-i\omega t} + \text{c.c.}, \quad (5)$$

where c.c. stands for the complex conjugate of the preceding term. The expansion coefficients $a_{l,\pm 1}^{(1)}$ result from the orthogonality of the $Y_{l,m}$ as

$$a_{l,\pm 1}^{(1)} = \frac{1}{4\pi} (1 - \epsilon^{-1}(\omega)) \frac{C(l) i \sqrt{l(l+1)}}{ka} \times (j_l(ka) + a_{E,\text{sc}}(l, \pm 1) h_l^{(1)}(ka)). \quad (6)$$

Then from the second or third power of the induced surface charge σ , acting as a driving source, one may determine the second (2ω) or third harmonic (3ω) field radiated by the cluster. Note the radiation emitted by this source is then modified by the linear response of the metal sphere and thus affected by Mie-resonances both in the incoming wave and the emitted higher harmonics.

2.2. The second and third harmonic generated by the surface charge

We calculate the radiated second or third harmonic from the second or third power of the induced surface charge σ . Hereby we include the modification of the emitted radiation by the linear response of the metal sphere, but neglect quantum mechanical effects arising from matrix elements [3], which are the same for large spheres and for plane surfaces. We expand now the powers of σ in spherical harmonics. Thus,

$$\sigma^n(\theta, \phi) = \frac{1}{2} \sum_{l=1}^{\infty} a_{l,m}^{(n)} Y_{l,m}(\theta, \phi) e^{-ni\omega t} + \text{c.c.} \quad (7)$$

The coefficients for σ are denoted by $a_{lm}^{(1)}$, those for σ^2 by $a_{lm}^{(2)}$ and those for σ^3 by $a_{lm}^{(3)}$. In addition to circularly polarized incident light, we also consider linear polarization, which is a linear combination of two circularly polarized waves of opposite helicity. The corresponding induced surface charge density is

$$\sigma(\theta, \phi) = \frac{1}{\sqrt{2}} (\sigma_+ + \sigma_-), \quad (8)$$

where the factor $2^{-1/2}$ results from the condition, that the linearly polarized incident wave should have the same intensity as a single circularly polarized wave. The sources of the second and third harmonic waves are in this case

$$\sigma^2(\theta, \phi) = \frac{1}{2} (\sigma_+^2 + 2\sigma_+\sigma_- + \sigma_-^2) \quad (9)$$

and

$$\sigma^3(\theta, \phi) = \frac{1}{2\sqrt{2}} (\sigma_+^3 + 3\sigma_+^2\sigma_- + 3\sigma_+\sigma_-^2 + \sigma_-^3). \quad (10)$$

Note, that in the case of linearly polarized light we obtain terms which mix contributions from waves with different helicities (e.g. $\sigma_+ \sigma_-$) in opposition to circularly polarized light which only gives pure terms ($\sigma^2 = \sigma_+^2$ and $\sigma^3 = \sigma_-^3$). This results in important differences in higher harmonic generation. Neglecting time-independent terms, we obtain

$$\begin{aligned} \sigma_+^2(\theta, \phi) &= \frac{1}{4} \sum_{l_1=1}^{\infty} \sum_{l_2=1}^{\infty} a_{l_1,1}^{(1)} a_{l_2,1}^{(1)} Y_{l_1,1} Y_{l_2,1} e^{-2i\omega t} + \text{c.c.}, \\ \sigma_-^2(\theta, \phi) &= \frac{1}{4} \sum_{l_1=1}^{\infty} \sum_{l_2=1}^{\infty} a_{l_1,-1}^{(1)} a_{l_2,-1}^{(1)} Y_{l_1,-1} Y_{l_2,-1} e^{-2i\omega t} + \text{c.c.}, \\ \sigma_+(\theta, \phi) \sigma_-(\theta, \phi) &= \frac{1}{4} \sum_{l_1=1}^{\infty} \sum_{l_2=1}^{\infty} a_{l_1,1}^{(1)} a_{l_2,-1}^{(1)} Y_{l_1,1} Y_{l_2,-1} e^{-2i\omega t} + \text{c.c.} \end{aligned} \quad (11)$$

Expanding σ^2 in spherical harmonics one obtains

$$\begin{aligned} \sigma_+^2(\theta, \phi) &= \frac{1}{2} \sum_{l=2}^{\infty} a_{l,2}^{(2)} Y_{l,2} e^{-2i\omega t} + \text{c.c.}, \\ \sigma_-^2(\theta, \phi) &= \frac{1}{2} \sum_{l=2}^{\infty} a_{l,-2}^{(2)} Y_{l,-2} e^{-2i\omega t} + \text{c.c.}, \\ \sigma_+(\theta, \phi) \sigma_-(\theta, \phi) &= \frac{1}{2} \sum_{l=1}^{\infty} a_{l,0}^{(2)} Y_{l,0} e^{-2i\omega t} + \text{c.c.} \end{aligned} \quad (12)$$

Because of the conservation of angular momentum, only the $a_{l,m}^{(2)}$ with $m=0, \pm 2$ are nonzero. They are

$$\begin{aligned} a_{l,2}^{(2)} &= \frac{1}{2} \sum_{l_1=1}^{\infty} \sum_{l_2=1}^{\infty} a_{l_1,1}^{(1)} a_{l_2,1}^{(1)} \int Y_{l,2}^* Y_{l_1,1} Y_{l_2,1} d\Omega, \\ a_{l,-2}^{(2)} &= \frac{1}{2} \sum_{l_1=1}^{\infty} \sum_{l_2=1}^{\infty} a_{l_1,-1}^{(1)} a_{l_2,-1}^{(1)} \int Y_{l,-2}^* Y_{l_1,-1} Y_{l_2,-1} d\Omega, \\ a_{l,0}^{(2)} &= \frac{1}{2} \sum_{l_1=1}^{\infty} \sum_{l_2=1}^{\infty} a_{l_1,1}^{(1)} a_{l_2,-1}^{(1)} \int Y_{l,0}^* Y_{l_1,1} Y_{l_2,-1} d\Omega. \end{aligned} \quad (13)$$

Similarly, we neglect terms oscillating at the frequency ω and obtain that

$$\begin{aligned} \sigma_+^3(\theta, \phi) &= \frac{1}{4} \sum_{l_1=1}^{\infty} \sum_{l_2=1}^{\infty} a_{l_1,1}^{(1)} a_{l_2,2}^{(2)} Y_{l_1,1} Y_{l_2,2} e^{-3i\omega t} + \text{c.c.}, \\ \sigma_-^3(\theta, \phi) &= \frac{1}{4} \sum_{l_1=1}^{\infty} \sum_{l_2=1}^{\infty} a_{l_1,-1}^{(1)} a_{l_2,-2}^{(2)} Y_{l_1,-1} Y_{l_2,-2} e^{-3i\omega t} + \text{c.c.}, \\ \sigma_+^2(\theta, \phi) \sigma_-(\theta, \phi) &= \frac{1}{4} \sum_{l_1=1}^{\infty} \sum_{l_2=1}^{\infty} a_{l_1,-1}^{(1)} a_{l_2,2}^{(2)} Y_{l_1,-1} Y_{l_2,2} e^{-3i\omega t} + \text{c.c.}, \end{aligned} \quad (14)$$

$$\sigma_+(\theta, \phi) \sigma_-^2(\theta, \phi)$$

$$= \frac{1}{4} \sum_{l_1=1}^{\infty} \sum_{l_2=1}^{\infty} a_{l_1,1}^{(1)} a_{l_2,-2}^{(2)} Y_{l_1,1} Y_{l_2,-2} e^{-3i\omega t} + \text{c.c.}$$

We expand σ^3 in spherical harmonics just like σ^2

$$\begin{aligned} \sigma_+^3(\theta, \phi) &= \frac{1}{2} \sum_{l=3}^{\infty} a_{l,3}^{(3)} Y_{l,3} e^{-3i\omega t} + \text{c.c.}, \\ \sigma_-^3(\theta, \phi) &= \frac{1}{2} \sum_{l=3}^{\infty} a_{l,-3}^{(3)} Y_{l,-3} e^{-3i\omega t} + \text{c.c.}, \\ \sigma_+^2(\theta, \phi) \sigma_-(\theta, \phi) &= \frac{1}{2} \sum_{l=1}^{\infty} a_{l,1}^{(3)} Y_{l,1} e^{-3i\omega t} + \text{c.c.}, \\ \sigma_+(\theta, \phi) \sigma_-^2(\theta, \phi) &= \frac{1}{2} \sum_{l=1}^{\infty} a_{l,-1}^{(3)} Y_{l,-1} e^{-3i\omega t} + \text{c.c.} \end{aligned} \quad (15)$$

From the conservation of angular momentum, we conclude that only the $a_{l,m}^{(3)}$ with $m = \pm 1, \pm 3$ are nonzero. They are

$$\begin{aligned} a_{l,3}^{(3)} &= \frac{1}{2} \sum_{l_1=1}^{\infty} \sum_{l_2=1}^{\infty} a_{l_1,1}^{(1)} a_{l_2,2}^{(2)} \int Y_{l,3}^* Y_{l_1,1} Y_{l_2,2} d\Omega, \\ a_{l,-3}^{(3)} &= \frac{1}{2} \sum_{l_1=1}^{\infty} \sum_{l_2=1}^{\infty} a_{l_1,-1}^{(1)} a_{l_2,2}^{(2)} \int Y_{l,-3}^* Y_{l_1,-1} Y_{l_2,2} d\Omega, \\ a_{l,1}^{(3)} &= \frac{1}{2} \sum_{l_1=1}^{\infty} \sum_{l_2=1}^{\infty} a_{l_1,-1}^{(1)} a_{l_2,-2}^{(2)} \int Y_{l,1}^* Y_{l_1,-1} Y_{l_2,2} d\Omega, \\ a_{l,-1}^{(3)} &= \frac{1}{2} \sum_{l_1=1}^{\infty} \sum_{l_2=1}^{\infty} a_{l_1,1}^{(1)} a_{l_2,-2}^{(2)} \int Y_{l,-1}^* Y_{l_1,1} Y_{l_2,-2} d\Omega. \end{aligned} \quad (16)$$

These results will be used now to determine the higher harmonic radiation fields.

2.3. Emission of higher harmonics

Having obtained the sources of higher harmonics, we now proceed to calculate the radiated power. A surface charge density results in a discontinuity of the radial component of the electric displacement over the surface of the sphere and continuity of the tangential component of the electric field over the surface. This can be written as $(\mathbf{D}_{\text{out}} - \mathbf{D}_{\text{in}}) \cdot \mathbf{n} = 4\pi\sigma^n(\theta, \phi)$, where $n=2$ for SHG and 3 for THG and $(\mathbf{E}_{\text{out}} - \mathbf{E}_{\text{in}}) \times \mathbf{n} = 0$. Because of the spherical symmetry only transverse magnetic waves are generated by the oscillating surface charge. Their frequencies have been discussed before. The boundary conditions require matching of the fields \mathbf{E}_{in} and \mathbf{E}_{out} . The fields outside the sphere are [10]

$$\begin{aligned} \mathbf{E}_{\text{out}}(\mathbf{x}) &= \sum_{l,m} \frac{A_E(l,m) \sqrt{l(l+1)}}{kr} h_l^{(1)}(kr) Y_{l,\pm m} \mathbf{n} \\ &+ \frac{A_E(l,m)i}{kr} \frac{\partial}{\partial r} [r h_l^{(1)}(kr)] \mathbf{n} \times \mathbf{X}_{l,\pm m} \end{aligned} \quad (17)$$

and inside the sphere as

$$\mathbf{E}_{\text{in}}(\mathbf{x}) = \sum_{l,m} \frac{B_E(l,m)}{\varepsilon k_1 r} \frac{\sqrt{l(l+1)}}{j_l(k_1 r)} Y_{l,\pm m} \mathbf{n} + \frac{B_E(l,m) i}{\varepsilon k_1 r} \frac{\partial}{\partial r} [r j_l(k_1 r)] \mathbf{n} \times \mathbf{X}_{l,\pm m} \quad (18)$$

where $k_1 = \sqrt{\varepsilon(n\omega)} k$ and $k = n\omega/c$. The boundary conditions yield the multipole coefficient of the radiated field

$$A_E(l,m) = \frac{C_1}{(\varepsilon - 1) C_2 + a(\varepsilon k C_3 - k_1 C_4)} \times \left(\frac{4\pi k a}{\sqrt{l(l+1)}} \right) a_{l,m}^{(n)}, \quad (19)$$

where $a_{l,m}^{(n)}$ is a coefficient in the expansions of σ^2 or σ^3 respectively. The constants C_1 – C_4 are given by

$$\begin{aligned} C_1 &= j_l(k_1 a) + k_1 a j_l'(k_1 a), \\ C_2 &= h_l^{(1)}(ka) j_l(k_1 a), \\ C_3 &= h_l^{(1)'}(ka) j_l(k_1 a), \\ C_4 &= h_l^{(1)}(ka) j_l'(k_1 a). \end{aligned} \quad (20)$$

The radiated power in terms of $c/8\pi$ and in units of the geometric cross section of the sphere, πa^2 , is given by

$$P = \frac{1}{\pi (ka)^2} \sum_{l,m} |A_E(l,m)|^2. \quad (21)$$

Comparing this result to the higher harmonic generation of a plane surface (see the appendix for details), we obtain the enhancement of higher harmonic generation by the sphere.

3. Results

For convenience, we relate the frequency ω of the incident radiation to the plasma frequency ω_p of the metal and use the reduced frequency $\Omega = \omega/\omega_p$ in our discussions. The dielectric function of the metal is $\varepsilon(\Omega) = 1 - 1/(\Omega(\Omega + i\gamma))$, where the damping γ takes the typical value of 0.01 in our calculations. Similarly the radius a of the sphere is given in terms of the wavelength of light $\lambda_p = 2\pi c/\omega_p$ at the plasma frequency and characterized by the parameter $q = 2\pi a/\lambda_p$.

Our calculation first begins with (6) for the expansion coefficients $a_{l,\pm 1}^{(1)}$ of σ , then we use (13) and (16) for the coefficients $a_{l,m}^{(n)}$ of σ^2 and σ^3 and finally the radiated second and third harmonic power is obtained from (19–21).

3.1. Second harmonic generation

Results for the frequency dependence of the radiated second harmonic power per unit cross section of the sphere

are given in Fig. 1 (for circularly polarized incident light) and Fig. 2 (linear polarization) for different sizes q . As a reference (long dashed line), we include the average power \bar{P} of the second harmonic generated at a plane surface (see appendix). Note, that this curve is multiplied by a factor of 100 to make comparison possible. For our discussion, we divide the frequency range into three regions: low-frequency region ($\Omega = 0.2 - 0.4$), Mie-resonance enhanced region ($\Omega = 0.4 - 0.7$) and high-frequency region

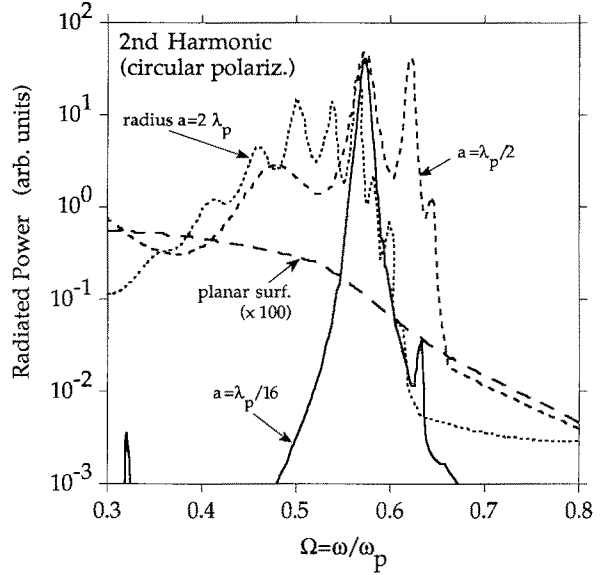


Fig. 1. Radiated power P of the second harmonic for circularly polarized incident light as a function of the reduced frequency $\Omega = \omega/\omega_p$ for three different sizes of the metal sphere: the solid line corresponds to a radius $a = \lambda_p/16$, the short-dashed line to $a = \lambda_p/2$ and the dotted line to $a = 2\lambda_p$. Here, $\lambda_p = 2\pi c/\omega_p$ is the wavelength of light at the plasma frequency ω_p of the metal. The long-dashed line refers to a planar surface and serves as a reference. Note, that the values of this curve have been multiplied by 100 to make a comparison possible

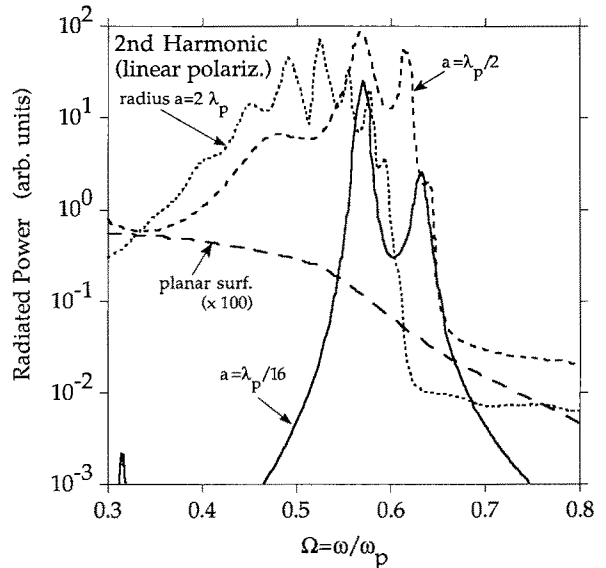


Fig. 2. The same as in Fig. 1 but for linearly polarized incident light

($\Omega = 0.7 - 1.0$). Each region has its own characteristic. Small spheres ($q \leq \pi/2$, solid line) generate significant second harmonic power only in a narrow region around the Mie-resonances ($\Omega \approx 0.58$). The power decreases rapidly for decreasing size. For larger spheres ($q \geq \pi/2$, short dashed line and dotted line), we obtain a second harmonic radiation for all frequencies with a strong enhancement in the range of the Mie-resonances. In the low frequency region ($\Omega \leq 0.4$) the radiated power first increases with increasing size q and reaches a maximum for $q \approx \pi$ (short dashed line). Thereafter, the power decreases for even larger sizes (e.g. $q = 4\pi$, dotted line). The maximum of the second harmonic is found for each cluster size in the range of the Mie-resonances. Note, retardation of the electromagnetic fields becomes important for larger sizes. This decreases the resonance frequency below $\Omega = 0.58$, which is only a lower limit for the resonances of very small spheres. The curves have many peaks because of various resonances at different multipolar modes l , which induce large local electric fields at the surface of the sphere and thus increase nonlinear optical properties. Above the highest resonance frequency the radiated power decreases very rapidly. Overall, the sphere of size $q = \pi$ gives the strongest second harmonic radiation. For linearly polarized incident light the radiated second harmonic power is generally higher. As an example, the single peak of the smallest sphere is divided in two, making it much broader. This is due to a radiating dipole term with $l = 1$ and $m = 0$ in the second harmonic, which comes from the product of two terms in the multipole expansion of the incident light, one with $l = 2$ and $m = +1$ and the other with $l = 1$ and $m = -1$ (or with inverse signs of the m). In contrast, for circularly polarized incident light m has either the value $+1$ or -1 . Thus $|m| = 2$ and $l \geq 2$ in the second harmonic, which only allows much less efficient quadrupole radiation. Thus the intensity is lower for circular incident polarization. An interesting question is the enhancement of the SHG in comparison to a plane surface. We give an estimate for the optimal size when $q = \pi$. For low frequencies there is practically no difference in the power of the second harmonic for the two types of polarization. The curves here coincide with the reference curve. Remembering that the values of the reference curve are multiplied by 100, we estimate an enhancement by a factor 100. For the Mie-resonance frequencies, we obtain an enhancement of approximately 2000 for circularly polarized incident light and 5000 for linearly polarized incident light. In the high frequency region the enhancement is only 100 times for circularly polarized incident light and an enhancement between 100 to 1000 times for linearly polarized incident light. We conclude that our calculation predicts an enhancement of about 5000 in the Mie-resonance frequency region, which is of the same magnitude as found in the experiments [1, 2].

3.2. Third harmonic generation

Our results for the third harmonic radiated power are shown in Fig. 3 for circularly and in Fig. 4 for linearly polarized incident light. As a reference, we include the average power of the third harmonic generated by a plane

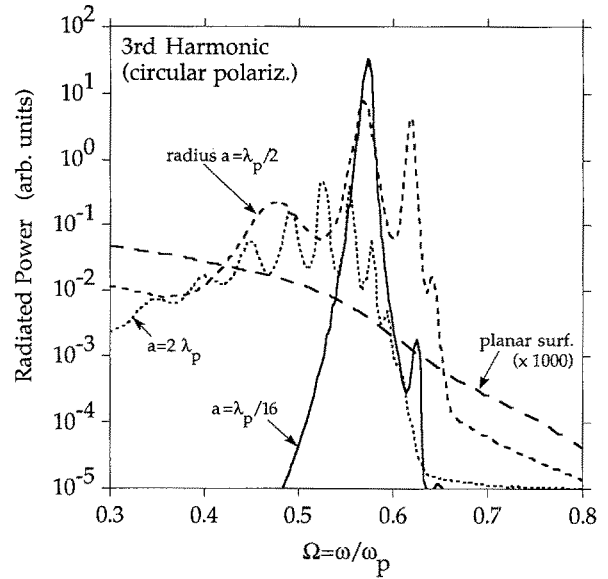


Fig. 3. Radiated power of the third harmonic for circularly polarized incident light and for the same sizes of spheres as in Fig. 1. The values of the reference curve has been multiplied by 1000 to make comparison possible

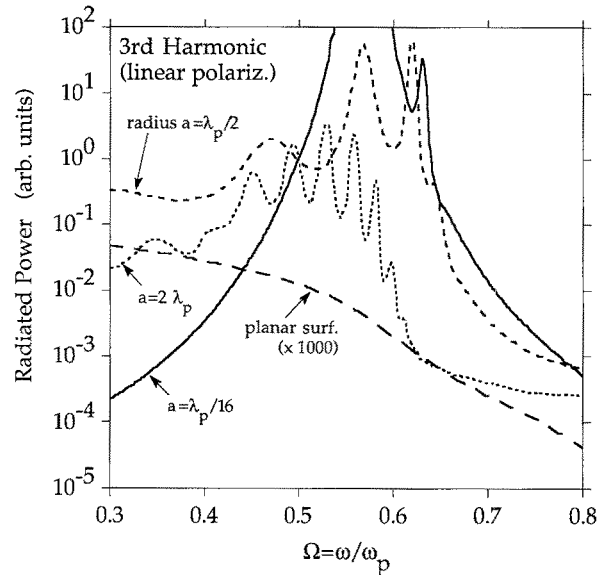


Fig. 4. The same as in Fig. 3 but for linearly polarized incident light

surface. Note that this curve is multiplied by a factor of 1000 to make a comparison possible. The same general behaviour is found here as for the second harmonic. Since the source of the third harmonic is the third power of the induced surface-charge density and the source of the second harmonic is the second power, one would expect that the enhancement of the third harmonic should be approximately equal to the enhancement of the second harmonic raised by the power of $3/2$. The sphere with size $q = \pi$ is also the optimal case for third harmonic generation. For low frequencies, we find an enhancement of approximately 5000, for Mie-resonance frequencies 200 000 and for high frequencies a factor 10 000, which is in good agreement with this qualitative argument. Cir-

cularly polarized incident radiation only allows octupole third order radiation in contrast to linear polarization which allows much stronger dipole radiation. This explains the large differences between Fig. 3 and Fig. 4.

4. Summary

In this work we have examined the second- and third harmonic generation of light by a metallic sphere. Mie theory has been used together with a phenomenological model for the higher harmonic generation. Note, we have determined the second harmonic $E_{(2)}$ of the local electric field at the surface of the sphere by effectively putting $E_{(2)} \cong \chi_2(\omega) E_{(1)}^2$, where $E_{(1)}$ is the local field due to the incident radiation and where we put $\chi_2(\omega) = \text{const.}$ Thus we have not taken into account quantum mechanical effects, which would cause an ω -dependence in χ_2 , which is the same for large metal spheres and for plane surfaces. Note, a similar relation as for $E_{(2)}$ holds for the third harmonic $E_{(3)}$. For comparison, an equivalent calculation is done for a planar surface using the same χ_2 . Mie resonances, which are not present at planar surfaces except for special geometries, enhance the local field $E_{(1)}$ at spherical surfaces and thus higher harmonics. On the other hand, small clusters radiate mainly as a dipole and higher multipole radiation is attenuated. This decreases the higher harmonic generation for very small cluster sizes and also results in important differences between linear and circular incident polarization.

We present results for spheres of sizes comparable to the wavelength $\lambda_p = 2\pi c/\omega_p$ of light at the plasma frequency ω_p of the metal. We obtain strongly enhanced higher harmonic radiation for larger spheres (radius $a > \lambda_p/2$) in a wide frequency range. The largest enhancement is obtained if the diameter roughly equals the wavelength of light at the plasma frequency of the metal. Linearly polarized incident light results in rather strong higher harmonics because of a radiating dipole term, which is not allowed for circular incident polarization. Small metallic spheres have other interesting nonlinear optical properties, such as selectively enhanced fourwave mixing. Using two circularly polarized incident waves of frequency ω_1 and ω_2 and the same helicity, we expect strong dipole radiation of frequency $2\omega_1 - \omega_2$ and $2\omega_2 - \omega_1$ because of third order nonlinearity. In this case the radiation of the sum frequencies $2\omega_2 + \omega_1$ and $2\omega_1 + \omega_2$ is only possible in the weaker octupole mode (this can be seen by considering the source $\sigma_+^2(\omega_1) + \sigma_+(\omega_2)$ in our model). Finally, our calculation gives an enhancement of second harmonic generation by a factor of about 5000 in comparison to plane metal surfaces. This is in good qualitative agreement with experiments on roughened metal surfaces.

It would be interesting to extend our work by also calculating $\chi_2(\omega)$ directly from an electronic theory. This might be necessary to understand better the differences between various metallic clusters (Na_n , Al_n , Ni_n etc.) and also between metallic- and semiconducting clusters.

One of the authors (D.Ö.) would like to thank Dr. P. Stampfli, Prof. K.H. Bennemann and Prof. E. Matthias at Freie Universität Berlin and A. Nyberg at the University of Göteborg for having had the possibility of doing this work at Freie Universität, Berlin.

Appendix.

Second and third harmonic generation by a plane surface

Here we consider only p -polarized incident waves with an electric field component, which is perpendicular to the surface and which induces surface charges. We use the usual expression for the transmission and reflection coefficients T and R at a plane interface. The induced surface charge density is

$$\sigma(\alpha) = \frac{1}{4\pi} \text{Re} \times \left[E \left(\sin \alpha + R \sin \alpha - T \frac{\sin \alpha}{\sqrt{\epsilon(\omega)}} e^{ikx \sin \alpha - i\omega t} \right) \right],$$

where α is the angle of incidence and E the amplitude of the incident radiation. As for the sphere, the powers of σ estimate the sources of higher harmonics. From the usual boundary conditions, we obtain the radiated electric field

$$|\mathbf{E}_{(n\omega)}(\alpha)| = \frac{4\pi\sigma^n(\alpha)}{\epsilon(n\omega) \frac{\sin \alpha \cos \alpha}{\sqrt{\epsilon(n\omega) - \sin^2 \alpha}} + \sin \alpha}.$$

Noting, that the higher harmonics are emitted in specular direction, we calculate the total radiated power, P , per surface area depending on the angle α . For a comparison with the higher harmonic generation of a sphere, we make an average of $P_{n\omega}(\alpha)$ over all angles α as defined by the geometry of a spherical surface. Note, that this also involves an average over the varying proportions of s - and p -polarization in the incident wave. The result is

$$\bar{P}_{(n\omega)} = \frac{1}{\pi} \int_0^{2\pi} \sin^n \phi d\phi \int_0^1 x |\mathbf{E}_{(n\omega)}^n(\arcsin x)| dx,$$

which is used as a reference for estimating the enhancement at a sphere.

References

1. Chen, C.K., Castro, A.R.B. de, Shen, Y.R.: Phys. Rev. Lett. **46**, 145 (1981); Boyd, G.T., Rasing, Th., Leite, J.R.R., Shen, Y.R.: Phys. Rev. **B30**, 519 (1984)
2. Wokaun, A., Bergmann, J.G., Heritage, J.P., Glass, A.M., Liao, P.F., Olson, D.H.: Phys. Rev. **B24**, 849 (1981)
3. Hache, F., Ricard, D., Flytzanis, C., Kreibig, U.: Appl. Phys. **A47**, 347 (1988)
4. Haglund Jr., R.F., Magruder III, R.H., Yang, L., Wittig, J.E., Zuh, R.A.: In: Physics and chemistry of finite systems: from clusters to crystals, Vol. II, Jena, P. (ed.), p. 1239. Dordrecht: Kluwer 1992
5. Hache, F., Ricard, D., Girard, C.: Phys. Rev. **B38**, 7990 (1988); Agarwal, G.S., Dutta Gupta, S.: Phys. Rev. **A38**, 5678 (1988);

- Stroud, D., Hui, P.M.,: Phys. Rev. B**37**, 8719 (1988); Kothari, N.C.: Phys. Rev. A**41**, 4486 (1990); Haus, J.W., Inguva, R., Bowden, C.M.: Phys. Rev. A**40**, 5729 (1989)
6. Martinos, S.S.: Phys. Rev. B**31**, 2029 (1985)
7. Mie, G.: Ann. Phys. (Leipzig) **25**, 377 (1908)
8. Russel, B.K., Mantovani, J.G., Anderson, V.E., Warmack, R.J., Ferrell, T.L.: Phys. Rev. B**35**, 2151 (1987)
9. Wang, C.C.: Phys. Rev. **178**, 1457 (1969)
10. Jackson, J.D.: Classical electrodynamics. (2nd ed.). New York: Wiley 1975